



Synthesis, characterization, and crystal structure analysis of 2-(2-hydroxy-3-methoxyphenyl)-1-(4-chlorophenyl)-4,5-diphenyl-1h-imidazole

M. Prabhuswamy, S. Viveka, M. Ramegowda, K. J. Pampa, G. K. Nagaraja & N. K. Lokanath

To cite this article: M. Prabhuswamy, S. Viveka, M. Ramegowda, K. J. Pampa, G. K. Nagaraja & N. K. Lokanath (2016) Synthesis, characterization, and crystal structure analysis of 2-(2-hydroxy-3-methoxyphenyl)-1-(4-chlorophenyl)-4,5-diphenyl-1h-imidazole, *Molecular Crystals and Liquid Crystals*, 629:1, 110-119, DOI: [10.1080/15421406.2015.1107811](https://doi.org/10.1080/15421406.2015.1107811)

To link to this article: <http://dx.doi.org/10.1080/15421406.2015.1107811>



Published online: 16 Jun 2016.



Submit your article to this journal [↗](#)



Article views: 44



View related articles [↗](#)



View Crossmark data [↗](#)

Synthesis, characterization, and crystal structure analysis of 2-(2-hydroxy-3-methoxyphenyl)-1-(4-chlorophenyl)-4,5-diphenyl-1H-imidazole

M. Prabhuswamy^a, S. Viveka^b, M. Ramegowda^c, K. J. Pampa^d, G. K. Nagaraja^b, and N. K. Lokanath^a

^aDepartment of Studies in Physics, University of Mysore, Mysore, Karnataka, India; ^bDepartment of Chemistry, Mangalore University, Mangalore, Karnataka, India; ^cPG Department of Physics, Govt. College (Autonomous) Mandya, Mandya, Karnataka, India; ^dDepartment of Studies in Microbiology, University of Mysore, Mysore, Karnataka, Karnataka, India

ABSTRACT

The substituted imidazole C₂₈H₂₁ClN₂O₂, was prepared via multicomponent reactions and the product crystallized using dimethylformamide. The structure of the compound was established by elemental analysis, Fourier transform infrared spectroscopy, thermogravimetric analysis, UV-visible, proton nuclear magnetic resonance spectroscopy, and single-crystal X-ray diffraction. The molecule is crystallized in the tetragonal crystal system with the space group P4₃2₁2 and with unit cell parameters $a = 12.246(4)$ Å, $b = 12.246(4)$ Å, $c = 31.781(2)$ Å, and $Z = 8$. The molecular and crystal structures of the title molecule are stabilized by the intramolecular interactions, O-H...N and C-H...N, and intermolecular interaction, C-H...O.

KEYWORDS

Crystallization; crystal structure; imidazole; intermolecular interactions; FTIR spectrum; Hirshfeld surface; multicomponent reaction; thermogram

Introduction

One of the major objectives of organic and medicinal chemistry is the design, synthesis of molecules, which are having highly therapeutic interest. Compounds containing imidazole moiety have many pharmacological properties and play important roles in biochemical processes. The imidazole ring system is the most important substructures found in a large number of natural products and pharmacologically active compounds [1]. For example, the amino acid histidine, the hypnotic agent etomidate [2], the antiulcerative agent cimetidine [3], the proton pump inhibitor omeprazole [4], the fungicide ketoconazole [5], and the benzodiazepine antagonist flumazenil [6] are imidazole derivatives. The potency and wide applicability of the imidazole pharmacophore can be attributed to its hydrogen bond donor-acceptor capability as well as its high affinity for metals, which are present in many protein active sites [7]. Trifena-grel is a 2,4,5-triaryl-1H-imidazole that reduces platelet aggregation in several animal species and humans [8].

Literature survey reveals the several methods for synthesizing them, mainly using nitriles and esters [9] as the starting substrates. Recently, there have been several methods reported in

CONTACT N. K. Lokanath  lokanath@physics.uni-mysore.ac.in  Department of Studies in Physics, University of Mysore, Mysore 570 006, India.

Color versions of one or more of the figures in the article can be found online at www.tandfonline.com/gmcl.

© Taylor & Francis Group, LLC

Table 1. Elemental analysis for $C_{28}H_{21}ClN_2O_2$.

Element	Experimental (%)	Calculated (%)
Carbon	74.29	74.25
Nitrogen	6.15	6.18
Hydrogen	4.68	4.67

the literature for the synthesis of 2,4,5-triaryl-1H-imidazoles from benzil/benzoin, aldehydes, and ammonium acetate using different catalysts [10,11]. These advantages offer an opportunity for a convenient and rapid library synthesis of substituted imidazoles. As a part of our ongoing studies into the crystal structure and utility of imidazoles [12] prompted us synthesize the some new substituted imidazole moiety and characterized by the single-crystal X-ray diffraction, elemental analysis, Fourier transform infrared (FTIR), TGA, $^1\text{H-NMR}$, etc.

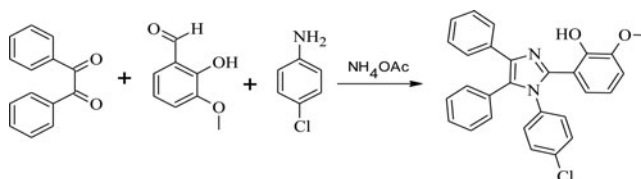
Experimental

Materials and methods

All chemicals were purchased Table 1 commercially and used without prior purification. IR spectra were recorded on a Shimadzu FTIR spectrophotometer in the range $400\text{--}4000\text{ cm}^{-1}$ using the KBr pellets. A TA-SQT Q600 thermogravimetric analyzer was used to obtain TGA curve under nitrogen atmosphere with a heating rate of $20\text{ }^\circ\text{C min}^{-1}$. The UV-visible (UV-Vis) spectrum was recorded in Shimadzu UV-2550 UV-Vis spectrophotometer. Elemental analysis was carried out by using VARIO EL-III (Elementar 10 Analysensysteme GmbH), melting points were determined in open capillary tube and were uncorrected. The proton nuclear magnetic resonance ($^1\text{H NMR}$) spectra were recorded on a Bruker AMX 400 NMR spectrometer with 5 mm PABBO BB-1H TUBES with tetramethylsilane as internal standard.

Synthesis of the compound 2-(2-hydroxy-3-methoxyphenyl)-1-(4-chlorophenyl)-4,5-diphenyl-1h-imidazole

The reaction progress was monitored by thin layer chromatography (TLC). After the completion of the reaction, benzil (10 mmol), orthovanillin (10 mmol), 4-chloroaniline (10 mmol), and ammonium acetate (12 mmol) were dissolved in boiling glacial acetic acid and refluxed for 6–8 hr. The reaction scheme is as explained in the Scheme 1. The reaction progress was monitored by TLC. After the completion of the reaction, the reaction mixture was poured into ice-water; the obtained compound was recrystallized from dimethylformamide. The product was obtained as white crystals with a yield of 87% and m.p. $182^\circ\text{C--}185^\circ\text{C}$.

**Scheme 1.**

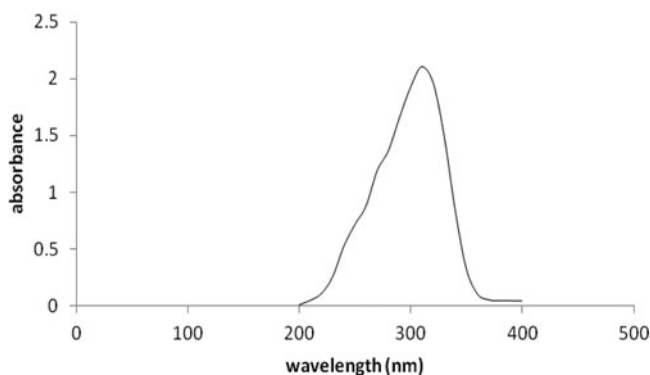


Figure 1. UV-Vis spectrum of the crystal.

Results and discussion

Elemental analysis

In order to confirm the chemical composition of the synthesized compound carbon (C), hydrogen (H), and nitrogen (N) analysis was carried out. The experimental and calculated percentages of C, H, and N were given in [Table 1](#). The differences between experimental and calculated percentages of C, H, and N were very close to each other and within the experimental errors. This confirms the formation of the product in the stoichiometries proportion.

UV-Vis spectral analysis

The UV-Vis spectrum of the compound was shown in [Fig. 1](#). The UV-Vis absorption spectra of the title compound were recorded in a methanol solvent.

The title compound exhibits absorption peaks in the UV-Vis region. The absorption peaks are observed at 309 nm due to the transition in the energy levels.

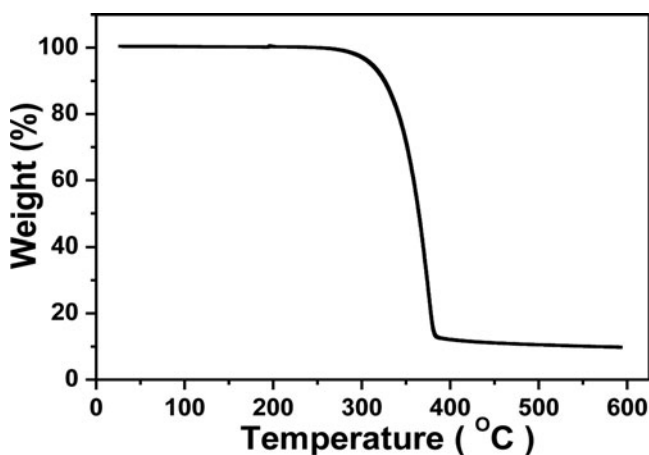


Figure 2. TGA curve of crystal.

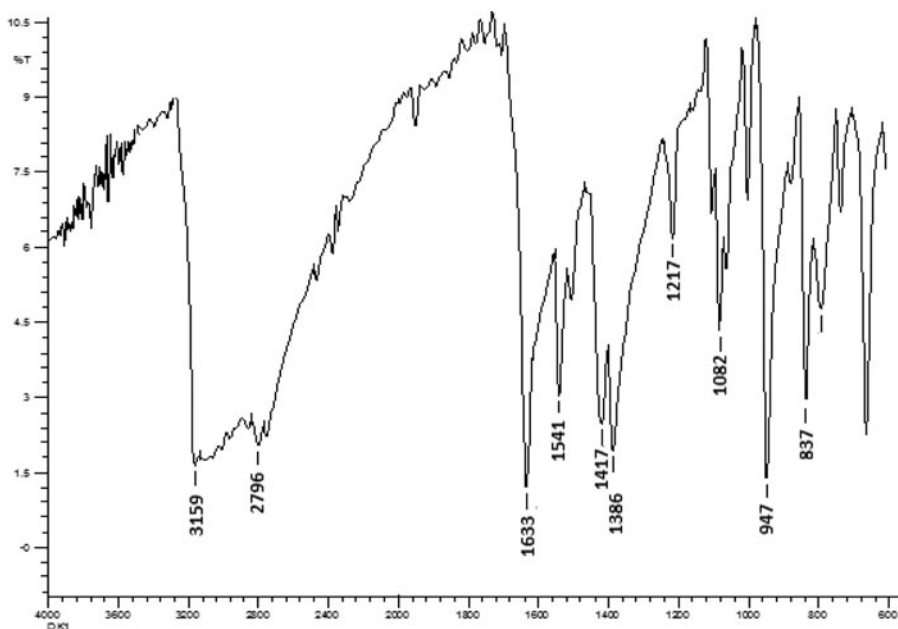


Figure 3. FTIR spectrum of the crystal.

Thermal gravimetric analysis (TGA)

The compound decomposes mainly in one stage on heating between 300 °C to 4000 °C as shown in Fig. 2. There was no much weight loss observed around 140 °C shows the absence of moisture in the crystal. A higher weight loss of around 90% occurs within 310 °C–385 °C. Above 400 °C, 10% of the residue was left out due to the charring of carbon. Above mentioned findings show the good thermal stability of the crystal.

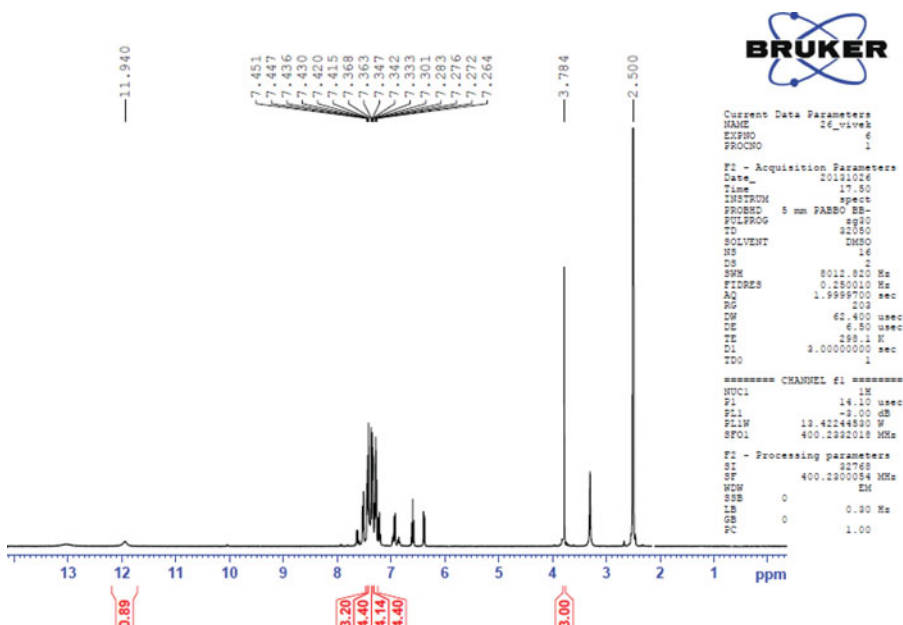


Figure 4. ¹H NMR spectrum of the crystal.

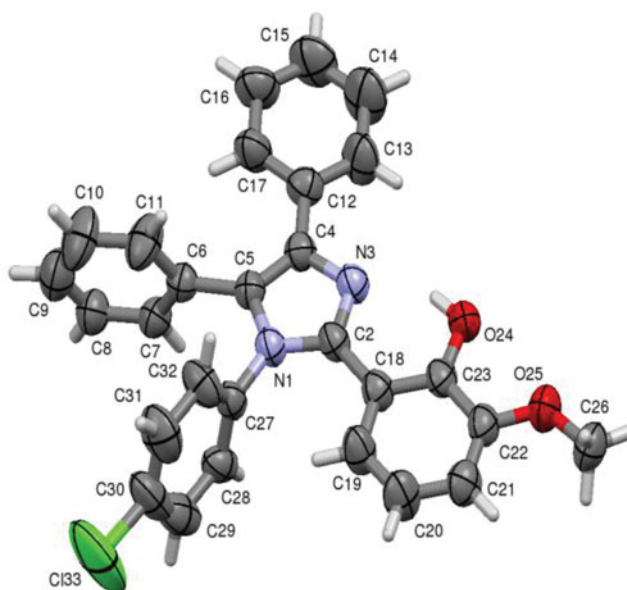


Figure 5. ORTEP of the molecule with numbering scheme for non-hydrogen atoms at 30% probability level.

FTIR spectral analysis

The FTIR spectrum of the crystal structure was shown in Fig. 3. The boardband at 3159 cm^{-1} corresponds to the O–H stretching vibration modes. The C–H stretching mode is superimposed in 2796 cm^{-1} . The 1633 and 1541 cm^{-1} were due to C = N and C = C stretching, respectively. The peaks observed at 1217 and 1082 cm^{-1} are due to C–O stretching vibration,

Table 2. Crystal data and details of structure refinement.

CCDC number	CCDC 96,0203
Empirical formula	$\text{C}_{28}\text{H}_{21}\text{ClN}_2\text{O}_2$
Formula weight	452.92 g mol^{-1}
Temperature	296 K
Wavelength	1.54178 \AA
Crystal system, space group	Tetragonal, $P4_32_12$
Unit cell dimensions	$a = 12.246(4)\text{ \AA}$ $b = 12.246(4)\text{ \AA}$ $c = 31.781(2)\text{ \AA}$
Volume	$4765.9(3)\text{ \AA}^3$
Z, calculated density	8, 1.262 Mg/m^3
Absorption coefficient	1.632 mm^{-1}
F_{000}	1888
Crystal size	$0.17 \times 0.19 \times 0.23\text{ mm}^3$
Theta ranges for data collection	$3.9\text{--}64.8^\circ$
Limiting indices	$-14 \leq h \leq 6, -14 \leq k \leq 14, -35 \leq l \leq 37$
Reflections collected/unique	27,799/3989 ($R_{\text{int}} = 0.058$)
Absorption correction	multiscan, $T_{\text{min}} = 0.705$ and $T_{\text{max}} = 0.769$
Refinement method	Full-matrix least-squares on F^2
Data/restraints/parameters	3989/0/300
Goodness-of-fit on F^2	1.02
Final R indices [$I > 2\text{sigma}(I)$]	$R1 = 0.056, wR2 = 0.153$
R indices (all data)	$R1 = 0.109, wR2 = 0.190$
Largest diff. peak and hole	0.26 and -0.22 e \AA^{-3}

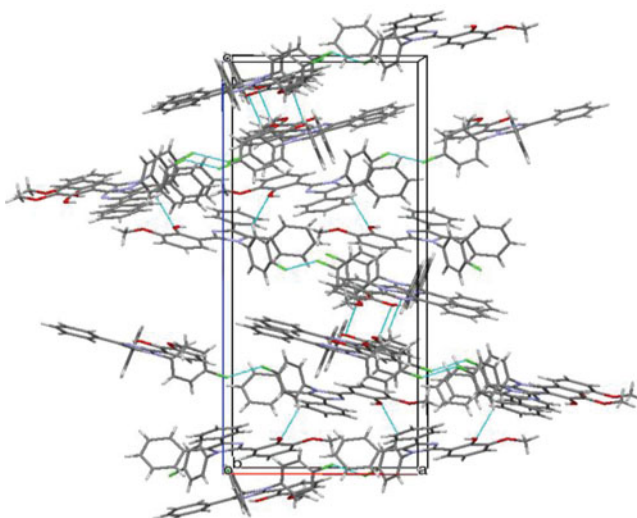


Figure 6. Packing of the molecules when viewed down along b axis. The dotted lines show C-H...O and Cl...Cl interactions.

1386 cm^{-1} assigned for the aromatic amines (C-N). The C-Cl stretching frequency assigned for the 837 cm^{-1} . The above mentioned functional group well agreement with the title compound.

¹H-NMR spectroscopy

The ^1H -NMR spectrum showed singlet at $\delta = 3.78$ ppm due to methoxy groups in the phenyl ring. The phenolic proton leads to a singlet of integration intensity equivalent to one hydrogen at 11.9 ppm. The multiplets appeared in the region $\delta = 7.26\text{--}7.45$ ppm integrating for 17 protons were due to aromatic protons. The ^1H NMR spectrum of the crystal structure was shown in Fig. 4.

Single crystal x-ray diffraction method

A white block shaped single crystal of dimension $0.17 \times 0.19 \times 0.23\text{ mm}^3$ of the title compound was selected for data collection. X-ray intensity data were collected for the title compound at temperature 296 K on Bruker X8 Proteum2 X-ray diffractometer [13] with X-ray generator operating at 45 kV and 10 mA, using $\text{CuK}\alpha$ radiation of wavelength $\lambda = 1.54178\text{ \AA}$. Data were collected with different settings of φ (0° and 90°), keeping the scan width of 0.5° , exposure time of 5 sec, and the sample to detector distance, 45.10 mm. A complete data set was processed using SAINT PLUS [14]. The structure was solved by direct methods and refined by full-matrix least squares method on F^2 using SHELXS and SHELXL [15]. All the non-hydrogen atoms were revealed in the first difference Fourier map itself. After several cycles of refinement, the final difference Fourier map showed peaks of no chemical significance and the residual is saturated to 0.056. The geometrical calculations were carried out using PLATON [16]. The molecular and packing diagrams were generated using the software MERCURY [17].

X-ray diffraction analysis revealed that the title compound is crystallized in the tetragonal crystal system with the space group $P4_32_12$ and with unit cell parameters $a = 12.246(4)\text{ \AA}$, b

Table 3. Selected bond lengths and bond angles (°).

C133–C30	1.726(8)	N1–C5	1.374(5)
O24–C23	1.344(6)	N1–C27	1.424(5)
O25–C22	1.373(6)	N3–C4	1.389(6)
O25–C26	1.414(7)	N3–C2	1.335(6)
N1–C2	1.374(4)		
C22–O25–C26	118.0(4)	N1–C5–C6	120.1(3)
C2–N1–C5	107.9(3)	N1–C5–C4	107.0(3)
C2–N1–C27	128.8(4)	O25–C22–C21	123.9(4)
C5–N1–C27	123.3(3)	O25–C22–C23	114.6(4)
C2–N3–C4	107.3(4)	O24–C23–C22	117.8(4)
N1–C2–N3	109.1(4)	O24–C23–C18	122.9(4)
N3–C2–C18	122.4(4)	N1–C27–C32	118.1(4)
N1–C2–C18	128.5(4)	N1–C27–C28	119.9(4)
N3–C4–C12	121.0(4)	C133–C30–C29	119.2(7)
N3–C4–C5	108.7(4)	C133–C30–C31	118.6(9)

$= 12.246(4) \text{ \AA}$, $c = 31.781(2) \text{ \AA}$, and $V = 4765.9(3) \text{ \AA}^3$. The ORTEP of the molecule with displacement ellipsoids drawn at 30% probability level is shown in Fig. 5. The crystal data and the details of the structure refinement are given in Table 2. Bond lengths and bond angles are given in Table 3. Table 4 lists the torsion angles.

Table 4. Torsion angles (°).

C26–O25–C22–C23	171.2(4)	C5–C6–C11–C10	– 176.9(5)
C26–O25–C22–C21	– 10.2(7)	C6–C7–C8–C9	– 1.6(9)
C5–N1–C2–C18	– 178.5(4)	C7–C8–C9–C10	1.8(11)
C5–N1–C2–N3	0.4(5)	C8–C9–C10–C11	– 0.9(12)
C2–N1–C5–C4	0.0(4)	C9–C10–C11–C6	– 0.3(11)
C27–N1–C2–N3	178.6(4)	C4–C12–C17–C16	176.8(5)
C27–N1–C2–C18	– 0.2(7)	C4–C12–C13–C14	– 177.2(6)
C27–N1–C5–C6	0.4(6)	C17–C12–C13–C14	0.4(9)
C2–N1–C27–C28	– 85.6(6)	C13–C12–C17–C16	– 0.8(9)
C2–N1–C27–C32	98.2(5)	C12–C13–C14–C15	– 0.8(12)
C5–N1–C27–C28	92.4(5)	C13–C14–C15–C16	1.6(12)
C5–N1–C27–C32	– 83.8(5)	C14–C15–C16–C17	– 2.0(10)
C2–N1–C5–C6	178.7(4)	C15–C16–C17–C12	1.7(10)
C27–N1–C5–C4	– 178.3(4)	C2–C18–C23–O24	2.7(6)
C2–N3–C4–C5	0.7(5)	C2–C18–C19–C20	178.6(5)
C2–N3–C4–C12	– 178.4(4)	C23–C18–C19–C20	– 0.2(8)
C4–N3–C2–N1	– 0.7(5)	C19–C18–C23–C22	0.2(6)
C4–N3–C2–C18	178.3(4)	C2–C18–C23–C22	– 178.6(4)
N1–C2–C18–C19	– 3.8(7)	C19–C18–C23–O24	– 178.4(4)
N3–C2–C18–C23	– 3.7(6)	C18–C19–C20–C21	– 0.6(9)
N1–C2–C18–C23	175.0(4)	C19–C20–C21–C22	1.3(8)
N3–C2–C18–C19	177.5(4)	C20–C21–C22–C23	– 1.3(8)
C12–C4–C5–N1	178.5(4)	C20–C21–C22–O25	– 179.8(5)
C12–C4–C5–C6	0.1(8)	O25–C22–C23–O24	– 2.1(6)
N3–C4–C12–C13	3.1(7)	O25–C22–C23–C18	179.2(4)
N3–C4–C12–C17	– 174.5(5)	C21–C22–C23–O24	179.2(4)
C5–C4–C12–C13	– 175.8(5)	C21–C22–C23–C18	0.5(7)
N3–C4–C5–N1	– 0.4(4)	N1–C27–C28–C29	– 177.8(4)
N3–C4–C5–C6	– 178.9(4)	C32–C27–C28–C29	– 1.8(7)
C5–C4–C12–C17	6.7(7)	N1–C27–C32–C31	176.9(5)
C4–C5–C6–C7	90.5(6)	C28–C27–C32–C31	0.8(8)
C4–C5–C6–C11	– 92.2(6)	C27–C28–C29–C30	1.9(8)
N1–C5–C6–C11	89.6(5)	C28–C29–C30–C133	177.8(5)
N1–C5–C6–C7	– 87.8(5)	C28–C29–C30–C31	– 1.1(10)
C5–C6–C7–C8	177.8(5)	C133–C30–C31–C32	– 178.9(5)
C7–C6–C11–C10	0.6(8)	C29–C30–C31–C32	0.0(11)
C11–C6–C7–C8	0.4(7)	C30–C31–C32–C27	0.2(10)

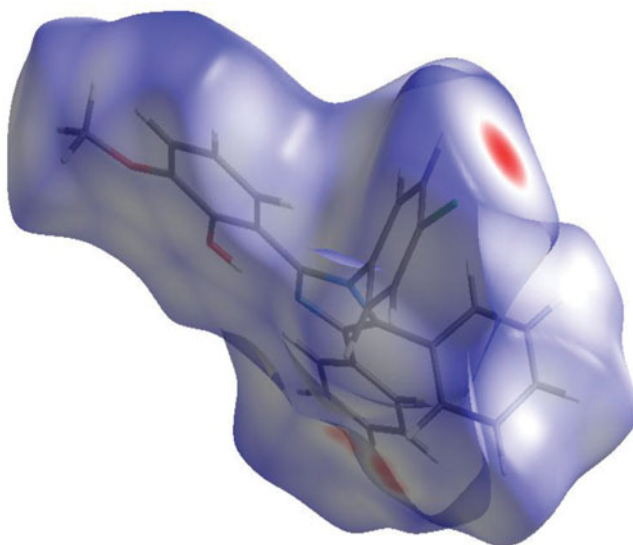


Figure 7. d_{norm} mapped on the Hirshfeld surface for visualizing the intercontacts of the molecule. Color scale between -0.050 au (blue) and 1.100 au (red).

The bond lengths and bond angles are comparable with those reported earlier for lophine (2,4,5-triphenyl-1H-imidazole) [18]. The imidazole ring N1/C2/N3/C4/C5 is planar as confirmed by the torsion angles of its segments. Torsion angles of $171.2(4)^\circ$ for the segment O25-C26 about C26-O25-C22-C23 and $179.2(4)^\circ$ for the segment C23-O24 about O24-C23-C22-C21 reflect that the methoxy and hydroxy groups are in an +anti-periplanar conformation with respect to the plane defined by the phenyl ring C18/C19/C20/C21/C22/C23.

The planes of the phenyl ring C6/C7/C8/C9/C10/C11 and chlorophenyl ring C27/C28/C29/C30/C31/C32 form dihedral angles of $89.9(3)^\circ$ and $84.7(3)^\circ$, respectively, showing that they lie in equatorial positions with respect to the plane described by the imidazole ring N1/C2/N3/C4/C5.

The dihedral angles of $4.9(3)^\circ$ and $4.5(2)^\circ$ formed, respectively, by phenyl ring C12/C13/C14/C15/C16/C17 and methoxyphenol ring C18/C19/C20/C21/C22/C23 reflect that they lie in axial positions with reference to the plane defined by the imidazole ring. The structure exhibits C-H...Cg interaction; C7-H7...Cg₄ (Cg₄ is the centroid of the ring C18/C19/C20/C21/C22/C23) with a C-Cg distance of $3.703(5)$ Å, H-Cg distance of 2.83 Å, C-H...Cg angle of 156° , and with a symmetry code $-1/2+x, 1/2-y, 1/4-z$. In the crystal lattice, the molecules exhibit intramolecular interactions, C-H...N and O-H...N forming a six-membered planar ring C2/N3/H24/O24/C23/C18 fused with the imidazole ring listed in Table 5. The crystal structure is further stabilized by C-H...O hydrogen bond interactions and Cl...Cl intercontacts with a distance of $3.098(4)$ Å (Fig. 6).

Table 5. Hydrogen bond geometry (Å, °).

D-H...A	D-H	H...A	D...A	D-H...A
O24-H24...N3	0.82	1.82	2.560(5)	149
C13-H13...N3	0.93	2.56	2.893(7)	101

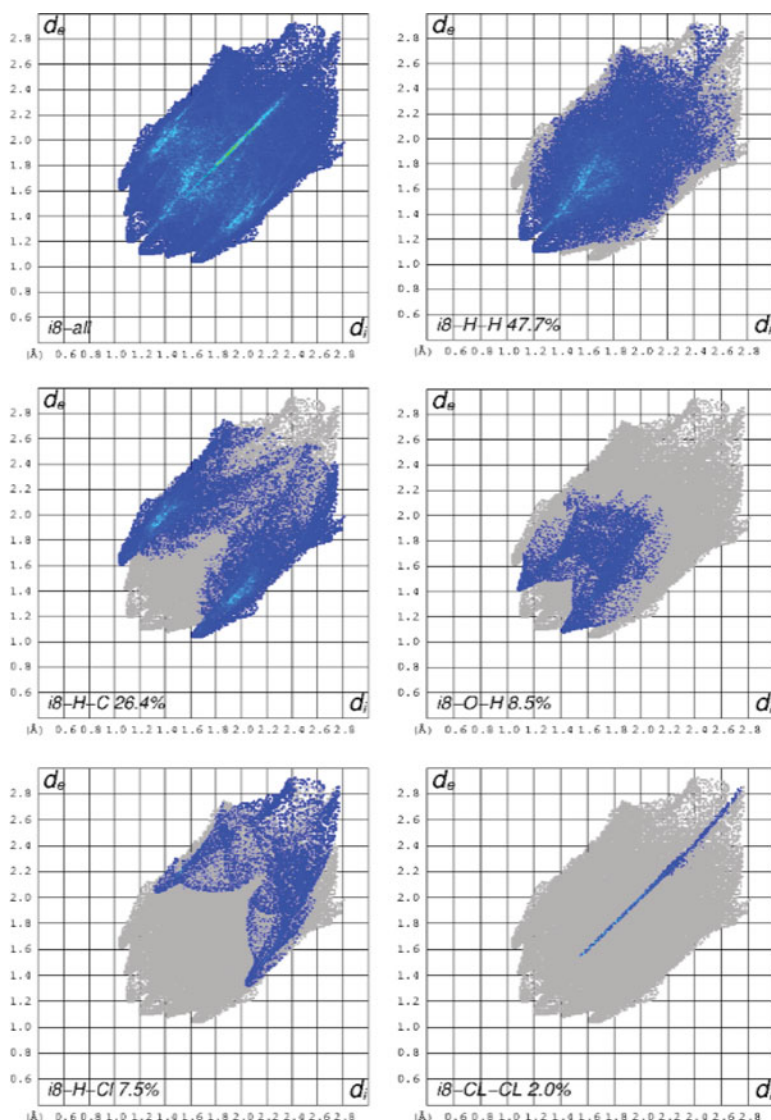


Figure 8. Fingerprint plots of the molecule.

Hirshfeld surface analysis

In order to visualize the intercontacts, Hirshfeld surface of the molecule was analyzed by the computational methods implemented in CRYSTAL EXPLORER [19]. The Hirshfeld surface and the fingerprint plots obtained due to the intercontacts between various atoms which are responsible for the formation of the Hirshfeld surface are shown in Figs. 7 and 8, respectively. The Hirshfeld surface analysis of the molecule confirms that there exists an intercontacts $\text{Cl}\cdots\text{Cl}$ which show up as a dark spot and fainter spots on the surface reflects $\text{C}\cdots\text{H}$ intercontacts.

It is evident from the fingerprint plots of the molecule that $\text{H}\cdots\text{H}$ (48%) intercontacts play a crucial role along with $\text{C}\cdots\text{H}$ (26%), $\text{O}\cdots\text{H}$ (8%), $\text{Cl}\cdots\text{H}$ (8%), and $\text{Cl}\cdots\text{Cl}$ (2%) intercontacts for the formation of Hirshfeld surface, showing that these intercontacts are responsible for the stabilization of molecular and crystal structures.

Conclusion

Single crystal was grown by the slow evaporation method. The elemental analysis confirms the formation of the compound in a stoichiometric ratio. The UV-Vis spectrum reveals the properties of the crystals. The FTIR and proton NMR spectrum reveals presence of the title compound. TGA was carried out to study the thermal behavior of the crystal. The single crystal X-ray diffraction studies show that the compound was crystallized in the tetragonal crystal system. The molecular and crystal structures are stabilized by the C-H...N, O-H...N, and C-H...O hydrogen bond interactions.

Acknowledgments

Authors thank the Institution of Excellence, Vigyana Bhavan, University of Mysore, Mysore, India, for providing single crystal X-ray diffraction facility to collect the data. The author V.S. gratefully acknowledge the UGC and DST-PURSE for the financial assistance and Mangalore University, USIC and MICROTONE center for their instrumental facilities. NMR research center Bangalore for the NMR spectrum.

References

- [1] Lambardino, J. G., & Wiseman, E. H. (1974). *J. Med. Chem.*, 17, 1182.
- [2] Wauquier, A., Van Den Broeck, W. A. E., Verheyen, J. L., & Janssen, P. A. J. (1978). *Eur. J. Pharmacol.*, 47, 367.
- [3] Brimblecombe, R. W. et al. (1975). *J. Int. Med. Res.*, 3, 86.
- [4] Tanigawara, Y. et al. (1999). *Clin. Pharmacol. Ther.*, 66, 528.
- [5] Heers, J., Backx, L. J. J., Mostmans, J. H., & VanCutsem, J. (1979). *J. Med. Chem.*, 22, 1003.
- [6] Hunkeler, W. et al. (1981). *Nature*, 290, 514.
- [7] Philips, A. P., White, H. L., & Rosen, S. (1982). *Eur. Pat. Appl.*, EP 58890.
- [8] Radziszewski, B. (1882). *Chem. Ber.*, 15, 1493.
- [9] Grimmett, M. R., & Katritzky, A. R. (1984). C.W. Rees (Eds.), 5, 457.
- [10] Sharma, G. V. M., Jyothi, Y., & Lakshmi, P. S. (2006). *Synth. Commun.*, 36, 2991.
- [11] Usyatinsky, A. Y., & Khmelnsky, Y. L. (2000). *Tetrahedron Lett.*, 41, 5031.
- [12] Prabhuswamy, M., Viveka, S., Kumar, S. M., Nagaraja, G. K., & Lokanath, N. K. (2013). *Acta Cryst.*, E69, 1006.
- [13] Bruker, (2012). APEX2, Bruker AXS Inc., Madison, Wisconsin, USA.
- [14] Bruker, (2012). SAINT PLUS, Bruker AXS Inc., Madison, Wisconsin, USA.
- [15] Sheldrick, G. M. (2008). *Acta. Cryst.*, A64, 112.
- [16] Spek, A. L. (1990). *Acta. Crystallogr. Sect. A.*, 46, C34.
- [17] Macrae, C. F. et al. (2008). *J. Appl. Cryst.*, 41, 466.
- [18] Yanover, D., & Kaftory, M. (2009). *Acta. Cryst.*, E65, o711.
- [19] Wolff, S. K. et al. (2012). CRYSTAL EXPLORER, Version 3.1.